AFRL-RV-PS-
TR-2011-0096

AFRL-RV-PS-
TR-2011-0096

NANOSCALE QUANTUM CONFINED STRUCTURES WITH PHOTON CONTROLLING CAVITIES

Sanjay Krishna

University of New Mexico
1313 Goddard Street SE
Albuquerque, NM 87106

13 July 2011

Final Report

AIR FORCE RESEARCH LABORATORY
Space Vehicles Directorate
3550 Aberdeen Ave SE
AIR FORCE MATERIEL COMMAND
KIRTLAND AIR FORCE BASE, NM 87117-5776

DTIC COPY
NOTICE AND SIGNATURE PAGE

This report is cleared for public release by the 377 ABW Public Affairs Office and is available to the general public, including foreign nationals. Copies may be obtained from the Defense Technical Information Center (DTIC) (http://www.dtic.mil).

AFRL-RV-PS-TR-2011-0096 HAS BEEN REVIEWED AND IS APPROVED FOR PUBLICATION IN ACCORDANCE WITH ASSIGNED DISTRIBUTION STATEMENT

//SIGNED//
LESLIE VAUGHN
Program Manager

//SIGNED//
PAUL D. LEVAN, Ph.D.
Technical Advisor, Space Based Advanced Sensing and Protection

//SIGNED//
B. SINGARAJU, Ph.D.
Deputy Chief, Spacecraft Technology Division
Space Vehicles Directorate

REPORT DOCUMENTATION PAGE

Form Approved
OMB No. 0704-0188

1. REPORT DATE *(DD-MM-YY)*	**2. REPORT TYPE**	**3. DATES COVERED** *(From - To)*
13-07-2011	Final Report	31 Jan 2007 – 15 Apr 2011

4. TITLE AND SUBTITLE
Nanoscale Quantum Confined Structures with Photon Controlling Cavities

5a. CONTRACT NUMBER
FA9453-07-C-0171

5b. GRANT NUMBER

5c. PROGRAM ELEMENT NUMBER
62601F

6. AUTHOR(S)
Sanjay Krishna

5d. PROJECT NUMBER
4846

5e. TASK NUMBER

5f. WORK UNIT NUMBER
299169

7. PERFORMING ORGANIZATION NAME(S) AND ADDRESS(ES)
University of New Mexico
1313 Goddard Street SE
Albuquerque, NM 87106

8. PERFORMING ORGANIZATION REPORT NUMBER

9. SPONSORING / MONITORING AGENCY NAME(S) AND ADDRESS(ES)
Air Force Research Laboratory
Space Vehicles Directorate
3550 Aberdeen Ave., SE
Kirtland AFB, NM 87117-5776

10. SPONSOR/MONITOR'S ACRONYM(S)
AFRL/RVSS

11. SPONSOR/MONITOR'S REPORT NUMBER(S)
AFRL-RV-PS-TR-2011-0096

12. DISTRIBUTION / AVAILABILITY STATEMENT
Approved for public release; distribution is unlimited. (Clearance # 377ABW-2011-0861, 13 Jun 2011)

13. SUPPLEMENTARY NOTES

14. ABSTRACT
The objective of the grant was to investigate novel quantum confined heterostructure coupled with photon controlling cavities. These would be used for developing high operating temperature (HOT) mid wave infrared (MWIR, 3 5 μm) and long wave infrared (LWIR) sensors. The heterostructures would be based on nanoscale self assembled quantum dots in a well design (DWELL). This effort will include a trade study to evaluate these technologies and a rigorous investigation of the performance parameters of these technologies. The final objective of this effort would be to demonstrate a 320 x256 MWIR focal plane array (FPA) operating at higher temperatures. There was a significant effort on developing quantum dot based focal plane arrays with plasmonic resonators. Promising results were obtained on plasmonic enhancement in 320x256 focal plane arrays.

15. SUBJECT TERMS
heterostructures, photoluminescence, crystallography

16. SECURITY CLASSIFICATION OF:			**17. LIMITATION OF ABSTRACT**	**18. NUMBER OF PAGES**	**19a. NAME OF RESPONSIBLE PERSON**
REPORT	**b. ABSTRACT**	**c. THIS PAGE**			Leslie Vaughn
Unclassified	Unclassified	Unclassified	Unlimited	40	**19b. TELEPHONE NUMBER** *(include area code)*

(This page intentionally left blank)

Table of Contents

LIST OF FIGURES

GLOSSARY

HOT	High operating temperature
MWIR	Mid-wave infrared (3~5 μm)
LWIR	Long-wave infrared (8~12 μm)
SAQD	Self-assembled quantum dots in a well design (DWELL).
DWELL	Quantum dots in a well
DDWELL	Quantum dots-in-a-double-well
FPA	Focal plane array
QWIP	Quantum well infrared photodetectors
QDIP	Quantum dot infrared detectors
SLS	Strained layer superlattices
QCSE	Quantum confined Stark effect
SKM	Stranski–Krastanow mode
MBE	Molecular beam epitaxy
RTB	Resonant tunneling barriers
IIL	Imaging interferometric lithography
FIB	Focused ion beam
SEM	Scanning electron microscope
FDTD	Finite difference time domain

(This page intentionally left blank)

1. SUMMARY

The objective of the grant was to investigate novel quantum-confined heterostructure coupled with photon controlling cavities. These would be used for developing high operating temperature (HOT) mid-wave infrared (MWIR, 3~5 μm) and long-wave infrared (LWIR) sensors. The heterostructure would be based on nanoscale self-assembled quantum dots in a well design (DWELL). This effort will include a trade study to evaluate these technologies and a rigorous investigation of the performance parameters of these technologies. The final objective of this effort would to demonstrate a 320 x256 MWIR focal plane array (FPA) operating at higher temperatures.

Overall Progress

We have made excellent progress on this project as determined by the number of publications (36 in total). In addition, there have been several M.S. and Ph.D. Students who have graduated based on this work. Here is a list of students who were partially supported by this effort.

Ph.D.

- Ram Attaluri, Ph.D. "Growth and Optimization of Dot-in-well (DWELL) Infrared Photodetectors" (Summer 2007) (Post doc at Lehigh University)
- Jonathan Andrews, Ph.D. "High Precision Radiometry Using an InAs/InGaAs Quantum Dot-in-a-Well Focal Plane Array, (Fall 2008) (Naval Research Lab)
- Chris Wilcox, Ph.D. "Atmospheric Turbulence Simulation Using a Liquid Crystal Spatial Light Modulator", (Fall 2009) (Naval Research Lab)
- Rajeev Shenoi, Ph.D., "Multispectral Plasmon Enhanced Quantum Dots-in-a-Double Well Infrared Detectors" (Fall 2010) (RPI)
- Vincent Cowan, "Type II SLS Based MWIR nBn Detectors", Ph.D. in progress (at AFRL/RVSS)

M.S.

- Nina Weisse-Bernstein, M.S., **with distinction**, "Investigation of the Feasibility of Creating Arbitrary Optical Transmission Using Surface Acoustic Waves and Surface Plasmons", Spring 2009 (LANL)

- Andrea Scott, M.S. “A Survey on Implementations of Integrated System Health Management (ISHM) for Air and Space Vehicles”, Fall 2008 (AFRL)
- Greg Bishop M.S. (Thesis), Spring 2008, “nBn Based Strain Layer Superlattice Detectors”. (Sandia National Lab)
- Jason Shelton M.S. (Thesis), **with distinction**, Summer 2008, “Series Connected Photovoltaic Arrays”. (Sandia National Lab)
- Eric Varley, M.S. (Thesis), Spring 2007, “Two color quantum dots in a well focal planer arrays”. (Sandia National Lab)
- Diana Jepson, M.S. (Thesis), Spring 2007, “1/f Noise measurements in HgCdTe Detectors”. (Air Force Research Lab)
- Michael Lenz, M.S. (Thesis) Summer 2007, “ Characterizing Spectral Response of Quantum Dots in a Well Focal Plane Arrays” (Sandia National Lab)

2. INTRODUCTION

MULTI-SPECTRAL infrared (IR) detection has major applications in the field of gas detection, identification of chemical and biological compounds, remote sensing and thermography. This capability is considered an integral part of third generation IR systems, along with large format arrays and higher temperature of operation. Multi-spectral detection can help in detection of targets, especially in low contrast and high clutter. Current multi-spectral systems make use of an external filter with a broadband focal plane array (FPA) or disperse the light on to several arrays. This approach however increases the cost of the arrays several fold. The use of external components such as filters or beam splitters increase the size of these systems and require complex optical alignment, as array sizes increase. As a result current 30–50 band multi-spectral arrays cost $10–$15 million. A limited multi-spectral capability;viz. dual color detection, can be achieved in arrays using back to back biased diodes or by asymmetric design of absorbing regions, enabling detection of multiple wavelengths by changing the bias polarity. Encoding of spectral and polarization information within the pixel can lead to large scale cost savings, reduced complexity and increased functionality of the arrays. The mid-wave infrared (MWIR) and long-wave infrared (LWIR) regions are of great

interest in imaging applications, due to the emission characteristics of objects near room temperature. Targets close to room temperature have high spectral content in these regimes and can be effortlessly identified using their spectral and polarization signatures. The major detector technologies currently existing in these regimes are bulk InSb in the MWIR, bulk HgCdTe in LWIR, and quantum well infrared photodetectors (QWIP) in LWIR. HgCdTe detectors have a high quantum efficiency and low dark currents; but due to problems inherent in the control of composition of the alloy, these detectors have a low yield. This increases the cost of HgCdTe detectors manyfold. InSb detectors are currently the dominant technology in MWIR, but need cooling to 77 K for their operation. Quantum dot infrared detectors (QDIP) and strained layer superlattices (SLS) are considered to be emerging technologies for third generation infrared detectors. These devices along with the QWIP, use transitions within quantum confined structures for infrared detection. They use mature growth and processing technologies associated with III-V compounds and this makes fabrication of large arrays using these technologies easier. We have used a variant of the QDIP, known as the dots-in-a-well (DWELL) infrared photodetector as the technology to demonstrate spectral tuning. In this technology quantum dots are embedded in a quantum well, and intersubband transitions in the conduction band of this system result in infrared absorption. The DWELL structure provides better control of the absorption wavelength when compared to QDIPs and provides a lower dark current. Dual color operation is also possible due to the nature of bound to bound and bound to continuum transitions that result in infrared absorption. As a result, the DWELL system exhibits a spectral response from 3–9 μm. This is very relevant for demonstration of spectral tuning, as it provides a broad wavelength range over which response of the cavity can be tuned. The DWELL system, using asymmetrically placed dots in a well can result in bias tunable spectral response due to quantum confined Stark effect (QCSE). Encoding of spectral information into a pixel has been attempted before by the use of Fabry–Perot cavities, which are epitaxially grown or by using microelectronic mechanical actuators (MEMS). Another approach is to use gratings etched on to the surface of the detector. This has resulted in improving performance of QWIPs in the LWIR region. Gratings etched into the active region couple incident light into higher order modes enabling higher absorption. The use of dielectric

and metallic deep etched photonic crystals have been attempted in the LWIR region, but the high aspect ratio needed in etching makes processing difficult. Here we present a novel method whereby the spectral and polarization response of a DWELL detector is tuned by coupling the absorption of the active region to the resonant modes of a surface Plasmon cavity integrated with the detector. This technique simplifies the processing required for the integration of the cavity without increasing the dark currents, is detector agnostic and can easily be transferred to a focal plane array.

2.1. Assumptions, Growth Procedures:

The detector samples used for demonstration of multi-spectral sensing have InAs quantum dots embedded in quantum wells as their active region with GaAs substrates. This design offers considerable advantages over systems based on quantum dots alone. Typically, solid state quantum dots are grown in the Stranski–Krastanow mode(SKM), using self assembly techniques. This method results in dots with varying sizes and hence it is difficult to control the operating wavelength of the detector. In a DWELL structure, transitions that result in infrared detection are from the ground state of the dot to a state in the well or in the continuum. This results in better control of operating wavelength for the system. The DWELL structures also exhibit a dual color response, with one peak in the MWIR and the other in the LWIR regions. This is due to the transitions from a state in the dot to quantum well and from the dot to the continuum. Bias tunable spectral response can be obtained in a detector based on DWELL design. This is done by placing quantum dots asymmetrically in wells, resulting in QCSE, leading to asymmetric spectral response with applied bias polarity . Two variants of the DWELL design were used to fabricate the detectors. The first structure consisted of quantum dots embedded in a single quantum well. The InAs dots were embedded in $In_{0.15}Ga_{0.85}As$ wells, with GaAs as the barrier material. The strain introduced due to the growth of the well and the quantum dots, limits the number of stacks of active region to 15 layers. Hence an alternate design, known as the dots-in-a-double-well (DDWELL) was developed that uses InAs dots embedded in $In_{0.15}Ga_{0.85}As$ /GaAs wells, with $Al_{0.10}Ga_{0.90}As$ as the barrier. The primary well for this system is GaAs as opposed to $In_{0.15}Ga_{0.85}As$ in the previous design. The $In_{0.15}Ga_{0.85}As$ layers are very thin, with 1 nm above and below the dots. Reduction in the amount of

strain inducing $In_{0.15}Ga_{0.85}As$ leads to growth of a higher number of active region stacks. The DDWELL design has 30 stacks of active region when compared to the DWELL design. This results in higher absorption cross-section of these devices, enabling their higher temperature operation. The use of DDWELL structures increases the operating temperature of the detectors, while maintaining its advantages like low dark current and spectral tuning. As to be discussed in Section III, the higher number of active region stacks results in a higher modal confinement of the resonant mode. A schematic representation of the conduction band of the DWELL design is shown in Fig. 1(a) and for the DDWELL design in Fig. 1(b).

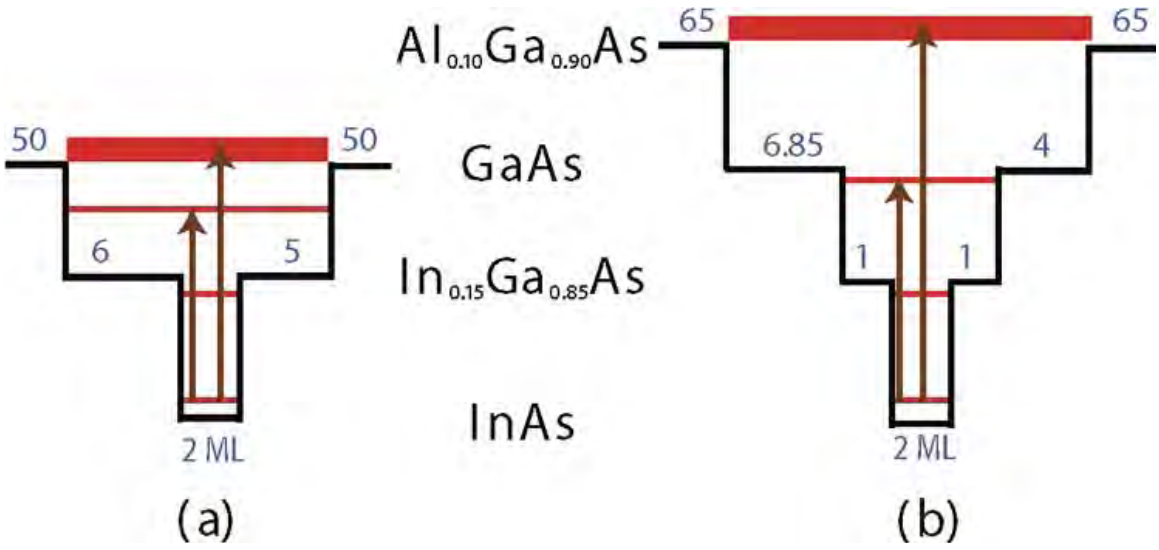

Fig. 1. Conduction band diagram of the DWELL and DDWELL designs. The dimensions of each layer are indicated in nm (blue) unless mentioned otherwise. The possible energy levels of the system (in red) and transitions resulting in infrared detection in the MWIR and LWIR windows are shown (in brown). The active region is 0.965 μm thick in DWELL sample and 2.45 μm in DDWELL sample. (a) DWELL. (b) DDWELL.

The detector structures were grown using solid source molecular beam epitaxy (MBE) using a V80 machine. The active region is sandwiched between top and bottom contacts consisting of n-doped GaAs, Si doped to $2x10^{18}$ cm^{-3}. An Al Ga As layer exists below the bottom contact layer, serving as a cladding layer to confine the resonant mode energy in the active region.

2.2. Fabrication Process:

Detector structures were processed in a class-100 cleanroom using standard techniques of mesa etching, passivation and contact metal deposition. The pixels consisted of top-illuminated 410x410 μm^2 mesas, with aperture diameters ranging between 25 and 300 µm. A thin layer of SiN was deposited as a passivation layer, followed by a contact metal and a thin plasmonic metal (Ti/Ag) evaporation by e-beam deposition. The plasmon metal covers the entire aperture of the detector, eliminating the detector response to IR light at this point. Care was taken to cover all excess area on the device by metal to reduce substrate scattering. Following this, three sets of samples were fabricated using e-beam lithography and dry etching: Sample A with DWELL active region, sample B and sample C with the DDWELL active region. Sample A and B have periodic square holes in a square lattice pattern, while sample C had lattice constants stretched in one direction and compressed in the orthogonal direction. Two control samples without the cavity or the plasmon metal were also prepared, control1 for sample A and control2 for samples B and C, as they have the same active region, to compare the effect of the cavity on the detector. The patterned samples and the control sample were part of the same growth and were processed together till the plasmon metal step, to eliminate variations in growth and processing. A top view of the fabricated detector is shown in Fig. 2(A) and an SEM image of the fabricated lattice is shown in Fig. 2(B).

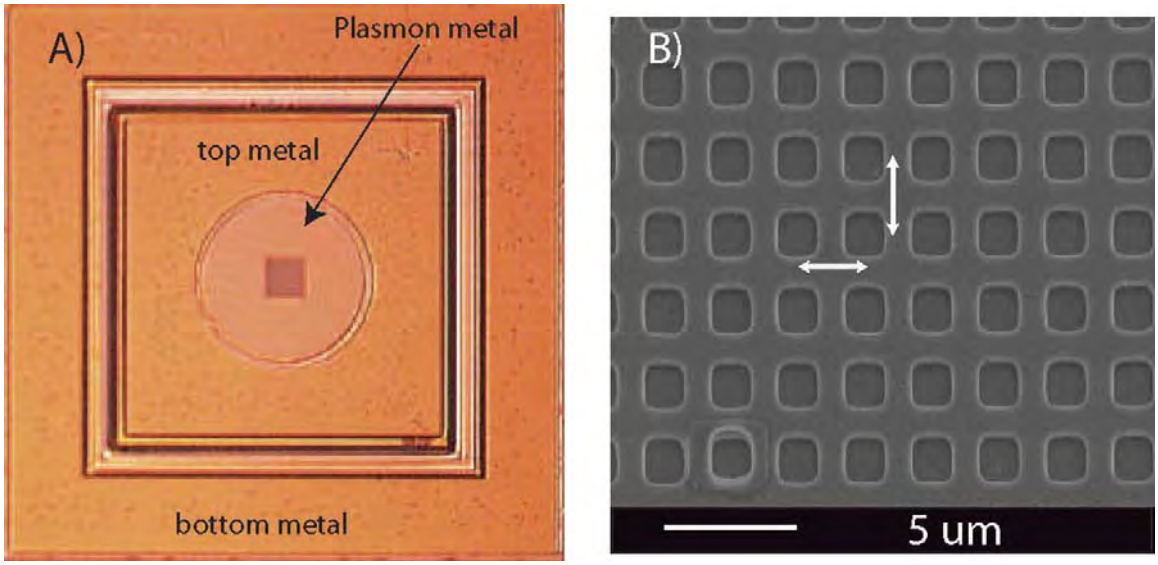

Fig. 2. Images of the fabricated plasmonic DWELL/DDWELL detector. (A) Optical image of the fabricated detector. The mesa, top metal, bottom metal and plasmonic metal can be observed. The square pattern at the center is the fabricated pattern. (B) Scanning electron microscopy (SEM) image of the etched pattern in the detector aperture. The pattern is a rectangular lattice with square holes, formed from a square lattice by stretching lattice constants in one direction and compressing it in the orthogonal direction.

3. RESULTS AND DISCUSSION

1st Year Detailed Technical Progress.

Two color InAs/InGaAs quantum dots in well (QDWELL) detectors were designed, grown, fabricated and characterized. Transmission electron microscopy images revealed that there were no defects in the device ensuring the good optical quality of the sample. Using standard cleanroom lithography techniques, such as wet and dry etching, metal evaporation and annealing, n-i-n detectors were fabricated. Devices with different active area dimensions were fabricated. The diameter of the devices varied from 25 μm to 300 μm. The devices were then wire bonded on to a chip carrier and delivered to Dr. Dave Cardimona's group at the Air Force Research Laboratory. Extensive blackbody and noise characterization was performed on these detectors.

Results

A two color quantum dot detector was realized and this was reported in Applied Physics Letter. A three color quantum dot detector operating in the MWIR (3.8 μm), LWIR (8.5 μm) and VLWIR (23.2 μm) was also designed grown and fabricated as shown in Fig 3.

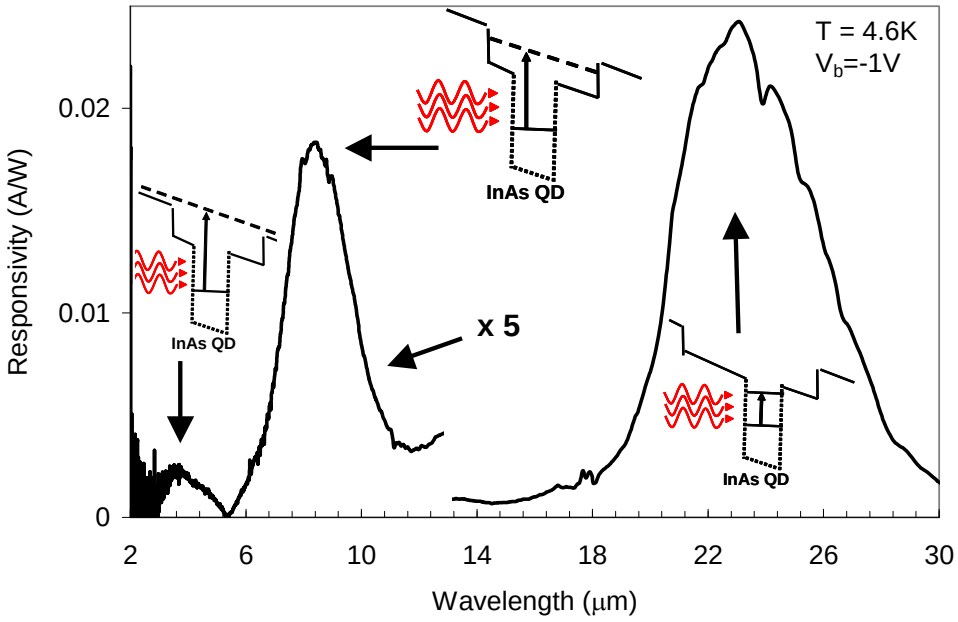

Fig. 3: Three color response from Quantum Dots in a Well detector. The inset shows the participating intersubband transitions.

Work is also in progress to realize a polarimeter based on quantum well infrared photodetectors. The details of this fabrication will be highlighted in the next report.

One of the PI's students working on this contract, Capt. Mario Serna, Jr. was selected as the finalist in the National Collegiate Inventors Competition.

Device Design and Fabrication

We grew a structure with a DWELL detector and an underlying waveguide consisting of a high Al composition $Al_{0.70}GaAs_{0.30}$ layer. The heterostructure schematic of the structure (UNM 2201) is shown in Fig. 4.

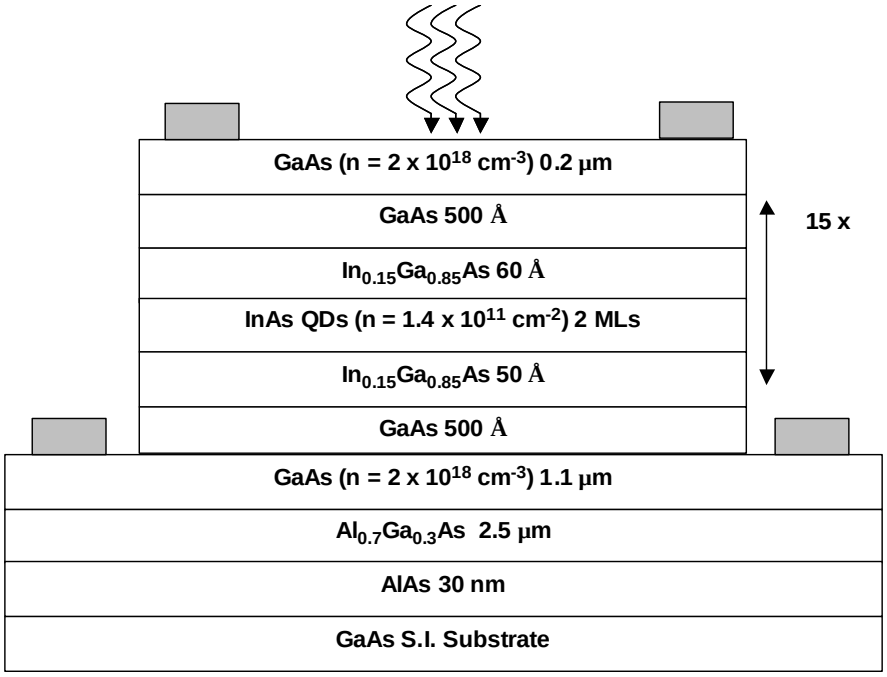

Fig. 4: Heterostructure schematic of the Dots in a Well detector that was grown by molecular beam epitaxy at UNM for the demonstration of plasmon assisted coupling.

One of the issues that we encountered while testing the previous batch of samples was the "residual" signal arising from the regions of the wafer that were not covered with the plasmonic metal. Hence we modified our mask sets in collaboration with Prof. Painter's group at Caltech. A new batch of devices was fabricated as shown below in Fig. 5 with no excess unexposed regions. Fig. 5 also shows some images from the plasmon structures that were fabricated at Caltech on devices that were grown and processed at UNM.

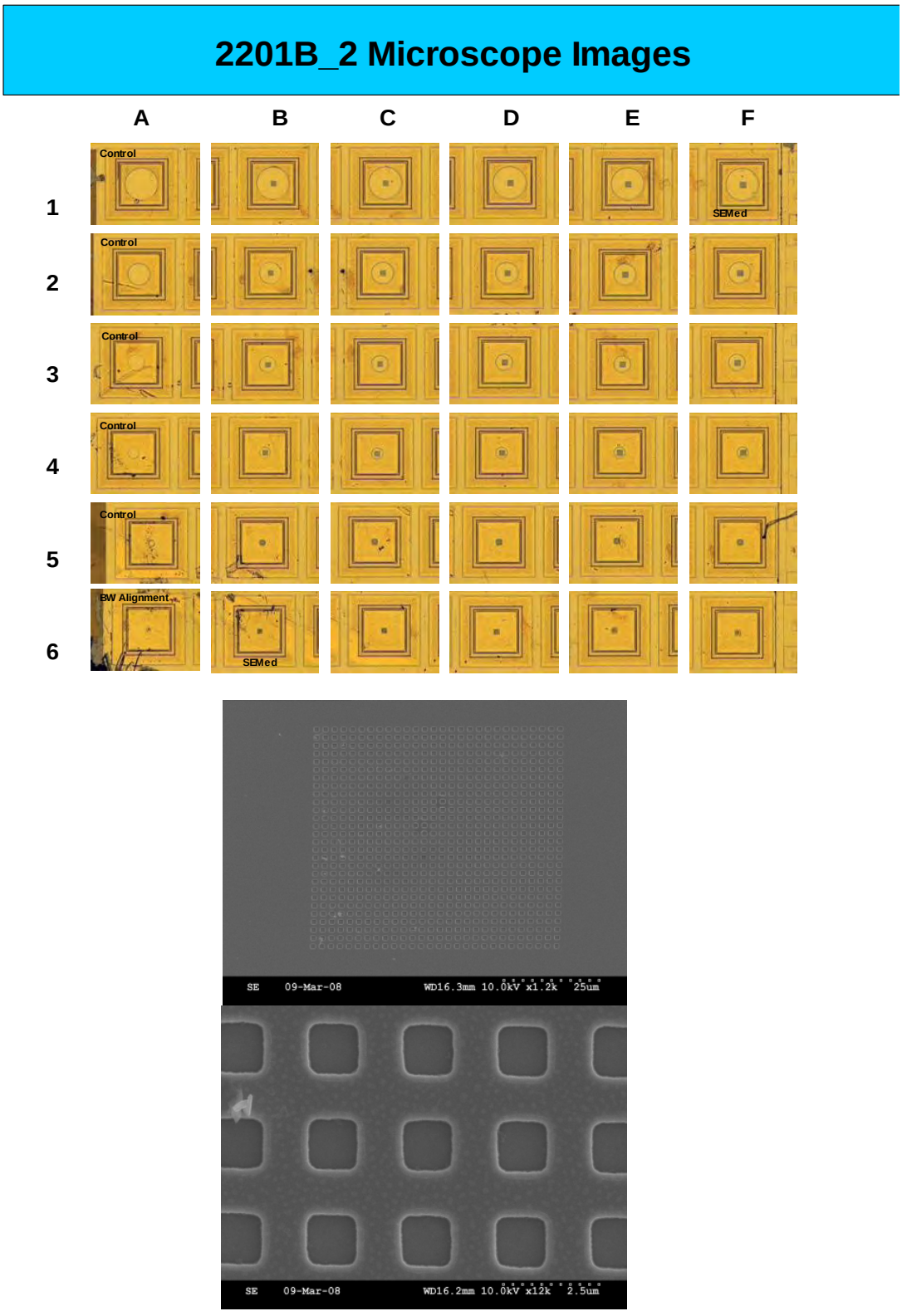

Fig. 5: Optical and SEM images of the devices that were developed at UNM in collaboration with Prof. Painter's group at Caltech.

In a parallel effort we have been working with Dr. Paul Alsing and graduate student, Ms. Casey Rhodes, to develop a theoretical understanding of the photonic crystal band structure. One of Prof. Painter's students, Ms. Jessie Roseberg, spent a week at UNM (March 10th-15th, 2008) with the PI's student, Mr. Rajeev Shenoi, to characterize the devices that were fabricated. We have obtained very encouraging preliminary results including the observation of resonances in the structure. We are currently working on understanding the data and comparing it with the theoretical model. In the next report, we will summarize the results of this study. In a parallel effort, we have been investigating alternate capping material to shape engineer the quantum dots to provide better 3D confinement and improve the operating temperature. Fig. 6 shows the first results from these structures are very encouraging and show operation at temperatures as high as 150K. We are currently studying the detailed figures of merit of these detectors.

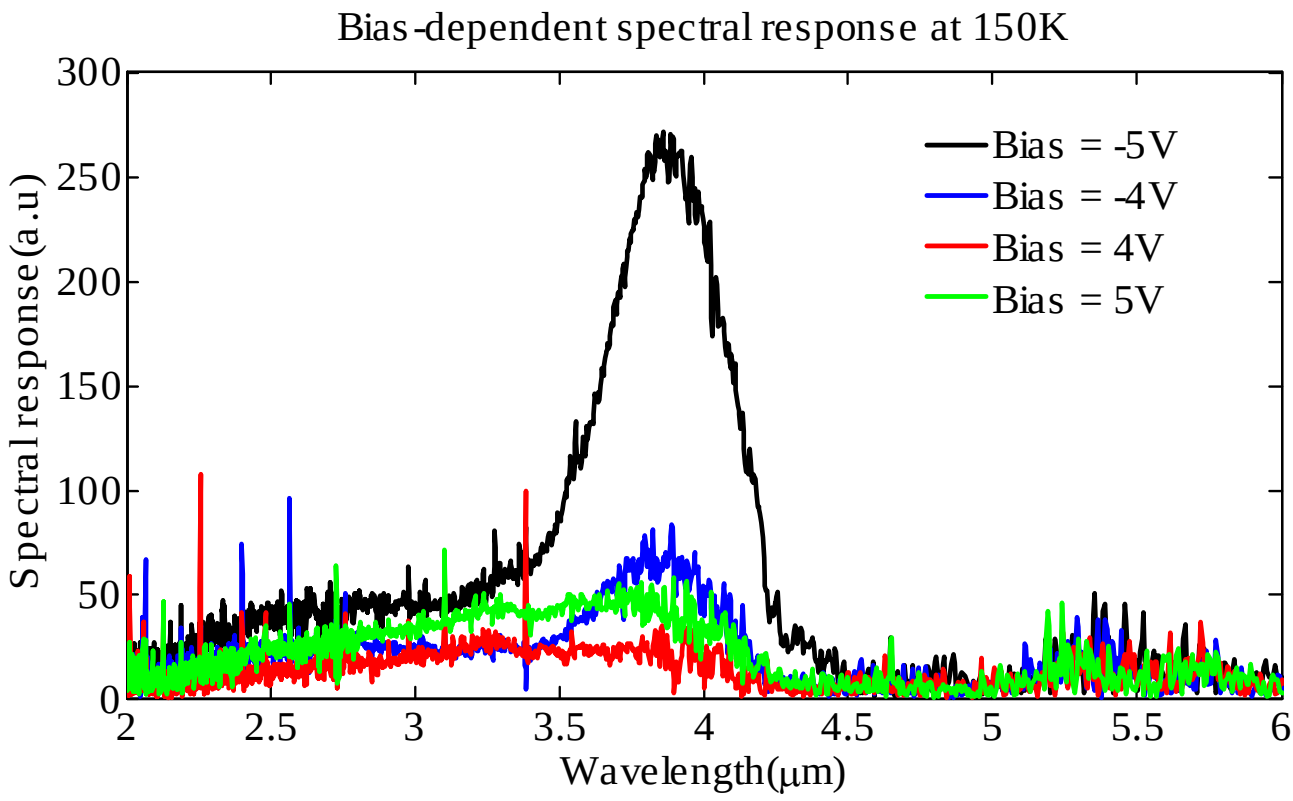

Fig. 6: Strong optical response from a heteroengineered dots in a well detector. Note that the response is at an operating temperature of 150K.

2nd year Detailed Technical Progress

Device Design and Fabrication

We have been investigating resonant tunneling devices using the DWELL design to decrease the dark current in quantum dots in a well detector. Designed Resonant Tunneling (RT) barriers allow energy-selective extraction of photoexcited carriers while blocking a continuum of dark carriers, resulting in an improvement in the signal-to-noise-ratio. Optical and electrical measurements demonstrate 2-4 orders of magnitude reduction in the device dark current in the RT-barrier device over a control sample without RT-barrier. Specific detectivity of $5x10^{10}$cm.$Hz^{1/2}W^{-1}$ also shows an improvement by a factor of 5, resulting in higher operating temperature for the device. Peak responsivity is 2.3A/W at -2.0V. Fig. 7 shows the simulation of the band structure and transmission probability of the resonant tunneling device.

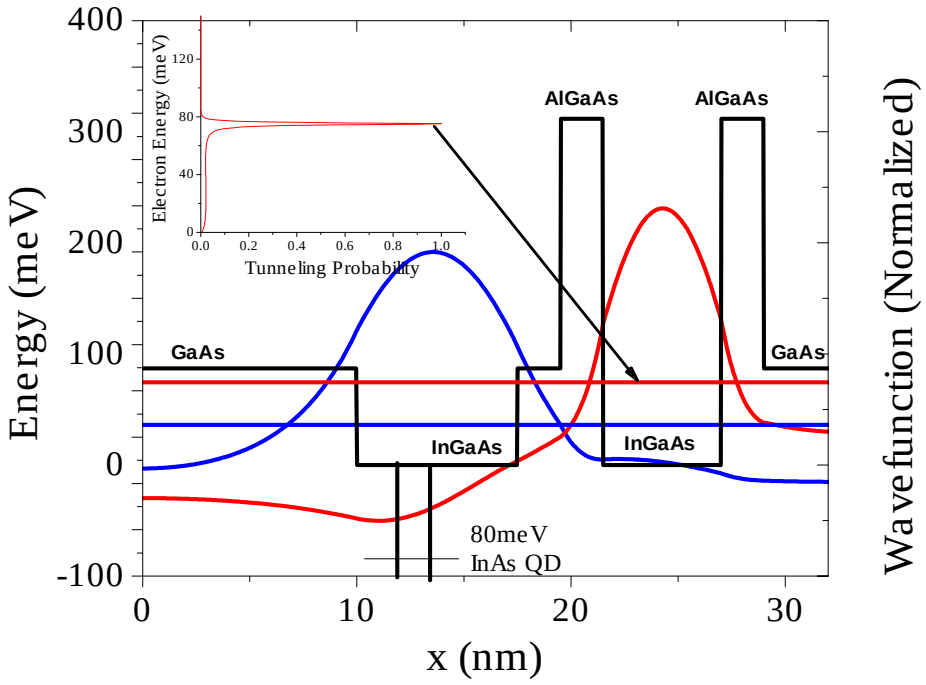

Fig. 7: Calculated eigen-energies and wavefunctions in RT-DWELL QDIP. The Resonance passband is aligned to the conduction band of GaAs. Inset shows a sharp tunneling probability

Quantum dot intersubband photodetectors (QDIP) are being widely researched as an emerging technology for low volume-high performance infrared detectors. Amongst the other competitive technologies, such as quantum well intersubband photodetectors (QWIP), Mercury-Cadmium-Telluride (MCT) based detectors and strained layer superlattice based detectors. QDIPs promise the lowest dark currents, higher operating temperature, large area uniform focal plane arrays [ref 6] and a tunable spectral response. Reduction in the dark current is possible because of the three dimensional confinement of carriers inside a quantum-dot giving rise to phonon bottleneck. The quantum dot-in-a-well (DWELL) type detectors, in which a quantum dot is placed inside a single or double quantum well, has been a topic of extensive research for the past few years. DWELL based detectors combine advantages of QDIPs, such as 3D confinement, with the advantages of QWIPs, such as ease of controlling the peak wavelength with repeatable, punch-in type growth recipes. The design of typical DWELL detectors involves a trade-off between lower dark current and higher peak wavelength. Typical dark current blocking layers, which offer triangular barriers, also block the photocurrent at higher wavelengths. In this letter, we propose the use of resonant tunneling (RT) barriers for DWELL detectors which remove the trade-off by clever barrier design, as they allow the designed energy levels to pass while blocking a continuum of energies, thereby reducing the dark current. Resonant tunneling barriers have been previously employed to reduce the dark current in QDIPs. With the RT-DWELL detectors, we demonstrate a significant 2-3 orders of magnitude improvement in the dark current over a so-called control sample. Control sample has the same structure and peak response wavelength as the RT-DWELL detector, but does not have the resonant tunneling barriers.

The samples were grown in a V-80 molecular beam epitaxy system, with an As_2 cracker source. The RT-DWELL sample has 10 stacks of InAs quantum dots in 7.5nm $In_{0.15}Ga_{0.85}As$ quantum well. The RT barrier on the top of the DWELL in each stack has 2nm GaAs, 2nm $Al_{0.3}Ga_{0.7}As$, 5.5nm $In_{0.15}Ga_{0.85}As$ and 2nm $Al_{0.3}Ga_{0.7}As$. There is an additional 50nm GaAs barrier between the two stacks. Control sample has a same structure except for the absence of the RT-barrier. The RT-barrier was designed in such a way that it allows the photocarriers excited from the dot in the positive bias to be extracted through resonant tunneling. As the pass-band of RT barrier is aligned to the

conduction band edge of GaAs, it also allows thermalized carriers to pass through in the negative bias. The calculated band diagram and energy-eigenvalues and wavefunctions are shown in Fig. 7. Calculated tunneling probability as a function of energy for an uncoupled RT-barrier is shown in the inset. Three point finite element method (FDM) was used to simulate the coupled well and RT-barrier structure, while the transfer matrix method was used to calculate the tunneling probability for RT-barriers. Results from both methods are in excellent agreement (within 2%) for the calculations of wavefunctions and energy eigenvalues. The above calculations simulate only 2D wavefunctions, that is, the quantum dot was not considered. As seen in the inset, the RT-barriers have a sharp transmission peak at the resonance energy, while it blocks majority of other energies. This allows lower dark current while maintaining a high peak wavelength.

The dark current in a DWELL device can be approximately modeled by a simplistic model based on the calculation of tunneling probability for the carriers from the quantum dot through the barriers. Surface dot density of $5x10^{10}$ cm^{-2}, inhomogeneous broadening of 40meV, saturation velocity of $2x10^{7}$ cm/s, electron mobility of $1000cm^{2}/V.s$ was assumed for the calculations. Fermi level was assumed to be located just above the ground state of the dot, as the dots are doped at approximately 1 electron per dot level. The model is accurate only for lower biases at relatively higher operating temperatures. Fig. 8 shows the measured dark currents for the two samples. As seen from the figure, 3-4 orders of magnitude improvement in the measured dark current in RT-DWELL samples at low temperatures is apparent as compared to the control sample. As the temperature increases, the improvement factor decreases to 2-3 orders of magnitude, but is still very significant. It can be seen that although the results match well for RT-DWELL devices, the measured dark current is actually higher than that predicted theoretically in the control sample. A practical consequence of reduction in the dark current is increase in operating bias range. This plays an important role in compensating for the loss of signal due to resonant tunneling barriers, as seen later. The reduction in the dark current is directly mapped into improvement in the operating temperature of the device, as seen from Fig. 8.

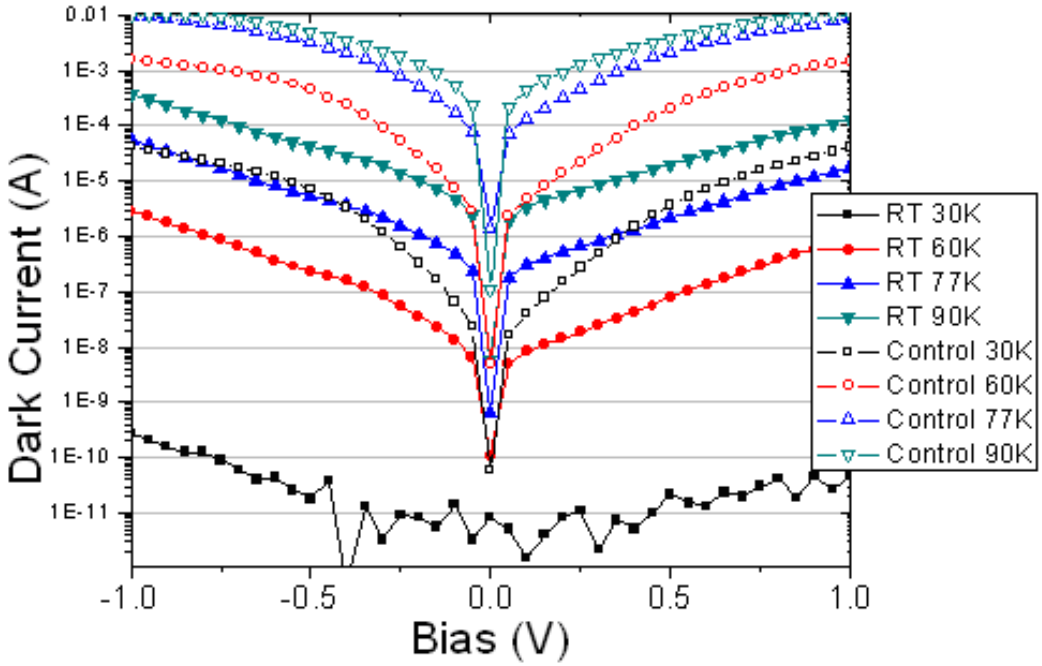

Fig. 8: Measured dark current for RT-DWELL (filled symbols) and a control sample (hollow symbols) 400x400μm^2 mesa device.

The normalized spectral response comparison at different temperatures shows the improvement in the signal to noise ratio, while keeping the peak wavelength approximately constant. Similar peak wavelength is useful for a fair comparison, as the dark current increases exponentially with the decrease in the intersubband energy difference, which, in turn, varies inversely with the peak response wavelength. Narrowing of the peak from 8-12μm to 10-12 μm, especially for the positive bias in RT-DWELL samples prove the existence of narrow pass-band resonance level which passes only a designed long-wavelength peak, which is believed to be originating from a bound to bound transition from dot to well, as depicted in Fig 7.

Resonant tunneling barriers, although decrease the dark current significantly; also decrease the photocurrent, thereby decreasing the responsivity. Fig. 9 shows the comparison of responsivity and specific detectivity of the two samples. The substrate scattering effects were neglected while calculating the responsivity. The responsivity is reduced by a factor of 2.5 at a given voltage. However, due to the higher operating bias range, the measured peak responsivity for RT-DWELL is actually higher than that of the

control sample. Secondly, since the R.M.S noise current is also reduced, the reduction in the responsivity at a particular bias is more than compensated such that there is a net improvement in the signal to noise ratio. This can be seen as an improvement in D* by a factor of 5. D* was calculated as

$$D^* = \frac{\sqrt{A_d \Delta f}\, R_v}{v_n} \left[\frac{\sqrt{\mathrm{cm}^2 Hz}}{W} \right]$$

where, A_d is the noise area of the device, which is 400μm x 400 μm for both the samples, Δf is the measurement bandwidth, R_v is the measured voltage responsivity, and v_n is the RMS noise voltage. Responsivity and D* were measured at 77K using a pour-filled dewar and a 900K blackbody source. The negative bias shows relatively larger response, as the carriers are thermalized before reaching the RT-barriers, and hence can pass through as the pass-band is designed to be very close to the GaAs conduction band. It should be noted that a simple device structure was used as a proof-of-a-concept for a RT-DWELL device and related theoretical calculations. A significant improvement in the device performance can be expected by the use of better designs for the parent sample, such as a double well structure which reduces the cumulative compressive strain per stack, allowing a greater number of stacks, thereby increasing the responsivity.

In conclusion, we present the design and characterization of a resonant tunneling barrier based DWELL samples. A 2-4 orders of magnitude improvement in the dark current of the device has been demonstrated for this device over a control sample. Closer analysis of spectral response clearly demonstrates the effect of resonant tunneling in these devices. Peak specific detectivity of ~5×10^9 cm.$Hz^{1/2}W^{-1}$ at 77K for the RT-DWELL device shows a factor of 5 improvement over the control sample despite a reduction in responsivity by a factor of 2.5 in this unoptimized structure. Reduction in responsivity can be easily compensated by higher operating bias range, which is a direct consequence of the reduction in the dark current by RT barriers. The peak responsivity is 2.3A/W at 77K. The results of this work were published in Applied Physics Letters (A Barve, S Shah, J Shao, T Vandervelde, R Shenoi, W Jang, and S Krishna, "Reduction in dark current using resonant tunneling barriers in quantum dots-in-a-well long wavelength infrared photodetector" Applied Physics Letters 93, 131115 (2008))

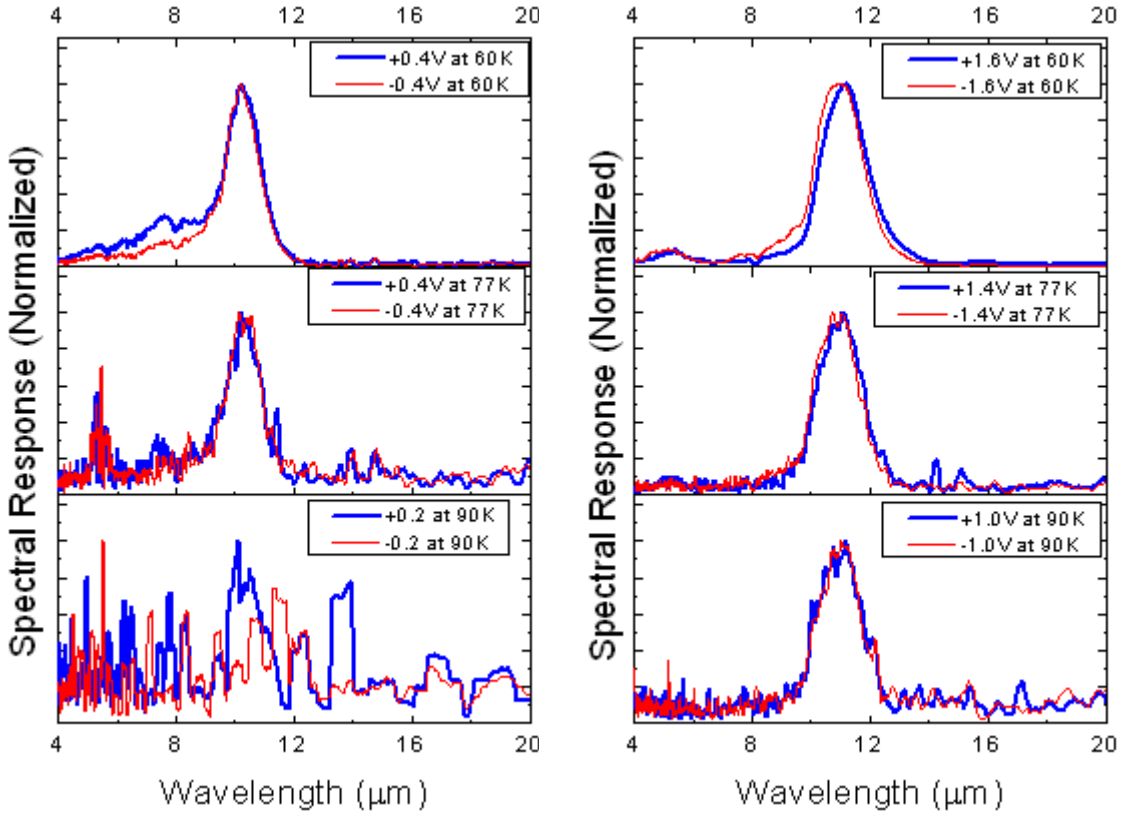

Fig. 9: Spectral response of a. Control sample b. RT-DWELL sample, at 30K, 60K, 90K (normalized to show the comparison between the two biases).

3rd year Detailed Technical Progress

As a part of this period, Prof. Krishna presented an invited talk at the "High Operating Temperature" Detector workshop organized by AFRL/RV (Dr. Dave Cardimona) and AFRL/RY (Dr. Michael Eismann) as a part of a NATO-SET workshop in Las Vegas, November 13th-14th 2008. We have been working towards improving the operating temperature of the detectors. An improvement to the dots-in-a-well design, known as the dots-in-a-double-well (DDWELL), was grown and fabricated during this period. In the DDWELL design, the quantum dots are embedded in $In_{0.15}Ga_{0.85}As/GaAs$ wells, as opposed to just $In_{0.15}Ga_{0.85}As$ wells. This helps in reducing the strain on the system, and enabling a higher number of active region layers. Detector structures with 30 active region stacks were grown using the DDWELL design, doubling the active region

thickness when compared to the DWELL design. The barrier thickness of these devices was optimized too, by varying the thickness of $Al_{0.10}Ga_{0.90}As$ used as the barrier.

Detector structures were fabricated using the DDWELL design, using standard cleanroom processing techniques of photolithography, dry etching and contact metal deposition. Detectors with varying aperture sizes were fabricated and extensive characterization was performed by measuring the spectral response, responsivity, detectivity and current-voltage characteristics of these devices.

DDWELL Results

The DDWELL samples show a lower dark current when compared to the DWELL structures, especially at higher bias voltages as shown in Fig.10. The dark current of the devices reduces with the barrier thickness and a barrier thickness of 65 nm was found to be optimal for this device.

The spectral response of these devices was characterized using a Fourier transform infrared spectrometer. With the improved design, the spectral response of these devices is recognizable up to a temperature of 140 K. A dual color response is observed with peaks at 8.7 and 9.4 microns as shown in fig. 11. The improvement in operating temperature is a result of the reduced noise in the DDWELL design.

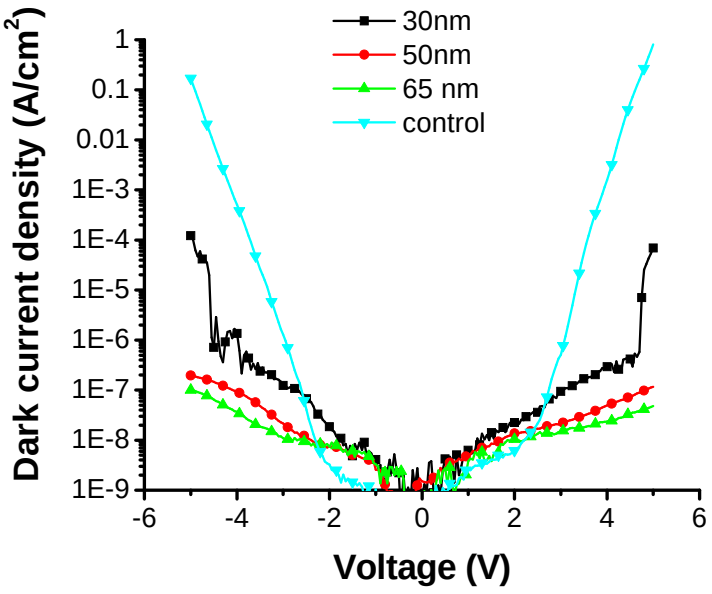

Fig. 10: Dark current density of DDWELL devices with varying barrier thickness and a DWELL control sample at 30 K.

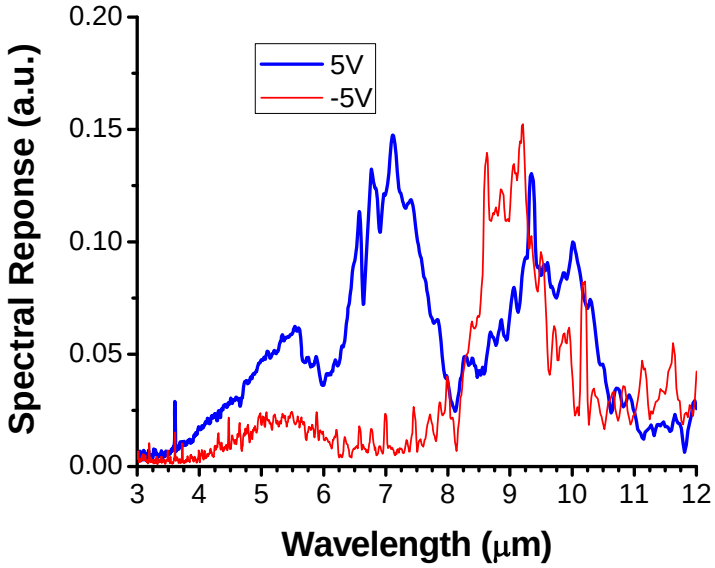

Fig. 11: Spectral response of the DDWELL sample at 120 K. A peak of 6.7 and 9.4 microns is seen at 5 V bias, while a peak of 8.7 microns is observed at -5 V bias.

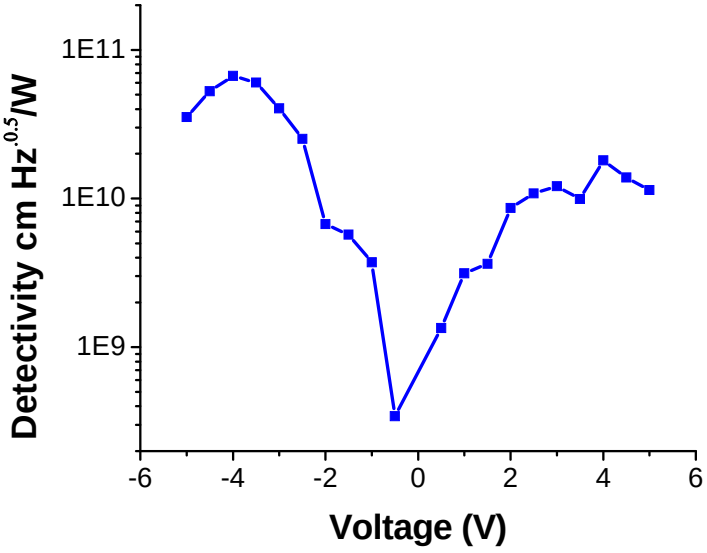

Fig. 12: Detectivity of DDWELL sample at 77 K. The peak detectivity of the 8.7 micron wavelength is 6.7×10^{10} Jones at -4 V bias.

The DDWELL design shows improved detectivity over the DWELL design as a result of the reduced noise and increased active region thickness. As shown in Fig. 12, a peak detectivity of 6.7×10^{10} Jones was observed at 77 K for a wavelength of 8.7 microns. This is an order of magnitude improvement over DWELLs and is comparable to the performance of QWIPs at this wavelength. We have made significant progress in this project. A set of single pixel devices was fabricated and a photon controlling cavity based on surface plasmons was integrated into these devices. The dots-in-a-well (DDWELL) design and the dots-in-a-double-well (DDWELL) were used for this purpose. The integrated cavity consisted of a square lattice with square holes in it. The cavity was created by patterning the surface of the detector and does not involve deep etching into the active region. A variation of this cavity where the lattice is stretched in one direction and compressed in the orthogonal direction was also fabricated. This results in the splitting of orthogonal modes into ones that are sensitive to the polarization of incident light. Simulations performed indicated an enhancement of the detector response by a factor of 5. The spectral response of the detector structures can be varied by varying the pitch of the pattern used, resulting in detectors with different peaks of absorption using the same active region which can be extended to fabricate multispectral focal plane arrays with pixel level encoding. Detector structures were fabricated using the DWELL and DDWELL design, using standard cleanroom processing techniques of photolithography, dry etching and contact metal deposition. The cavity was integrated using e-beam lithography and dry etching. Patterns were fabricated with response peaks in the mid-wave infrared (MWIR) and long-wave infrared (LWIR) region. Extensive characterization was performed by measuring the spectral response, responsivity, detectivity and current-voltage characteristics of these devices.

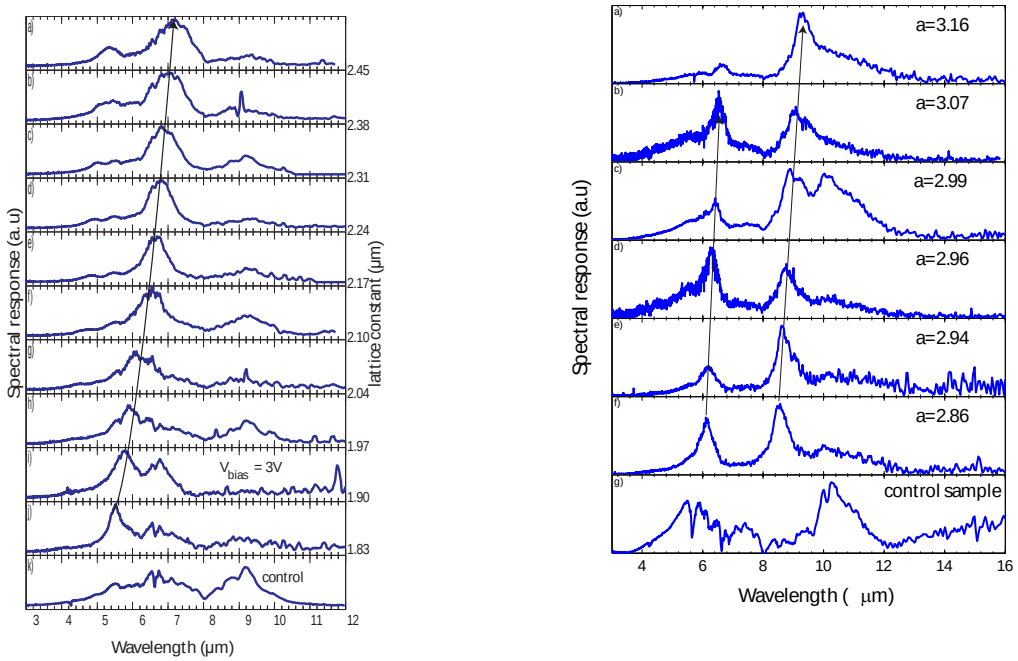

Fig. 13: Spectral tuning of wavelength with the pitch of the fabricated pattern. **(a)** Tuning in DWELL devices: Tuning from 8.5 to 9 microns is achieved. **(b)** Tuning in DDWELL devices: Spectral response is changed from 5.5 to 7.2 μm. All measurements were performed at 30 K.

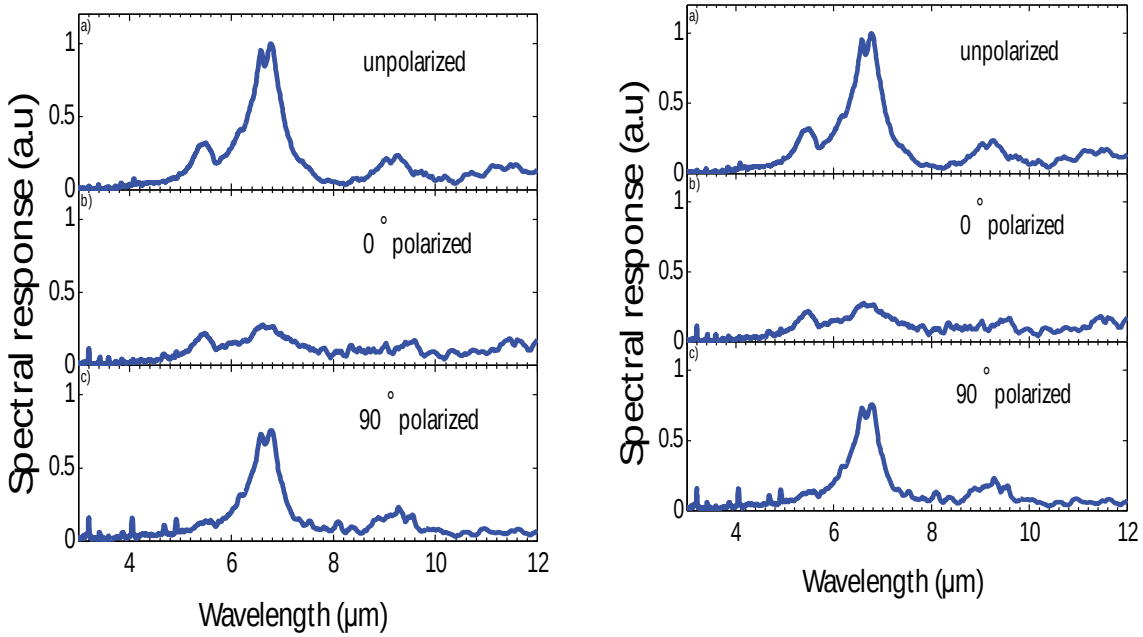

Fig.14: Polarization dependent spectral response of patterned DDWELL samples with a stretched/compressed lattice at 30 K. A peak of 6.6 μm is seen at 5 V bias, which is sensitive to incident polarization

.

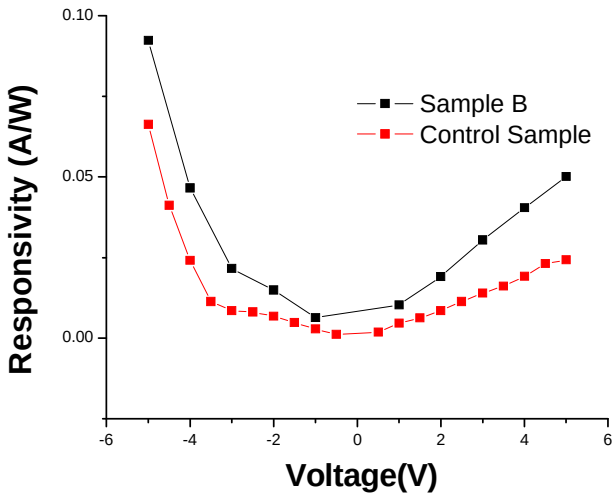

Fig. 15: Responsivity of a patterned DDWELL sample at 77 K with that of the unpatterned control sample. An enhancement of the responsivity is obtained as a result of the integration of the cavity with the detector.

DDWELL Results

The patterned samples show a significant change in spectral response when compared to the unpatterned ones. DDWELL samples show a lower dark current when compared to the DWELL structures, especially at higher bias voltages as shown in Fig. 13. The dark current of the devices reduces with the barrier thickness and a barrier thickness of 65 nm was found to be optimal for this device. Fig.14 shows the spectral response of the devices was measured using a Fourier transform infrared spectrometer and the polarization response was measured using a wire grid polarizer.

The integration of the cavity with the detector improves the response, as a result of the enhanced confinement and coupling of the incident radiation to the modes of the cavity. As shown in Fig. 15, an enhancement of the responsivity is obtained. This enhancement has been observed across a wide range of wavelengths and peak enhancement of 5.5 was observed at a wavelength of 7.2 μm. The integration of the cavity with the detector improves the response, as a result of the enhanced confinement and coupling of the incident radiation to the modes of the cavity. As shown in Fig. 16, an enhancement of the

responsivity is obtained. This enhancement has been observed across a wide range of wavelengths and peak enhancement of 5.5 was observed at a wavelength of 7.2 μm

4th Year Detailed Technical Progress

During the past few months, significant effort was made to understand the origin and limitations of spectral tuning in dots-in-a-well (DWELL) detectors using surface plasmons. Efforts were made to develop alternate cavity designs that would focus light, enabling better detector performance. The in-house fabrication facilities were significantly improved through use of the Quanta 3D dual beam Scanning Electron Microscope (SEM) / Focused Ion Beam (FIB) at the UNM Department of Earth and Planetary Sciences. This tool allowed us to develop and improve fabrication of features with sub-micron precision, essential for cavities in the infrared region. A process was developed to control the feature sizes and etch depth precisely. A fabricated pattern using the FIB is illustrated in Fig .16. Attempts were also made to make use of imaging interferometric lithography (IIL) for fabrication of high throughput sub-micron feature sizes, for fabrication of cavities at the wafer level.A modeling framework was developed to understand the origin of spectral tuning. Using spatial and spectral localization of modes, two types of modes, plasmonic and waveguide, were found to exist within the detector structure, depending on the active region thickness and the geometric pattern used. It is possible to selectively excite modes in a detector structure using a set of metallic holes in a square lattice and a set of square posts on a square lattice. The selective excitation of these modes in these structures will go a long way towards understanding the effects of these modes in infrared detectors. Detector structures were fabricated using the DWELL design, using standard cleanroom processing techniques of photolithography, dry etching and contact metal deposition. The cavity was integrated using e-beam lithography and dry etching at the Centre for Integrated Nanotechnologies at Sandia National Laboratories. Patterns were fabricated with response peaks in the mid-wave infrared (MWIR) and long-wave infrared (LWIR) region. Extensive characterization was performed by measuring the spectral response, responsivity, detectivity and current-voltage characteristics of these devices. An image of the fabricated pattern is shown in Fig.17

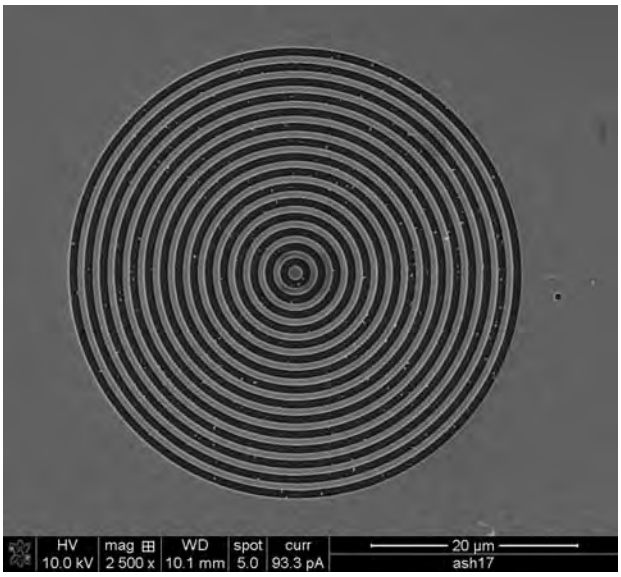

Fig 16: Fabricated bull's eye pattern using metal deposition and FIB milling. A gallium beam at 30 KV was used to etch this pattern onto a GaAs substrate

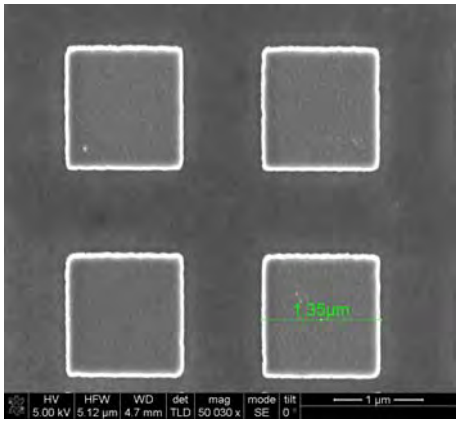

Fig 17: Image of fabricated metal post pattern using e-beam lithography and metal deposition**.**

Results

The absorption of metallic post samples was modeled using finite difference time domain (FDTD) techniques. A plot of the mode profile in the y-z direction for the fundamental mode of absorption is shown in Fig. 18. It indicates that the electric field is fundamentally concentrated away from the metal-semiconductor interface, and has a minimal interaction with the fabricated pattern, indicating a waveguide like nature. Detector structures fabricated with metallic post samples show a clear suppression of the long-wave peak in spectral response when compared to the unpatterned ones, as shown in Fig. 19. Future efforts will be directed towards understanding the properties of these modes and to fabricate to demonstrating spectral tuning effects in an infrared focal plane array.

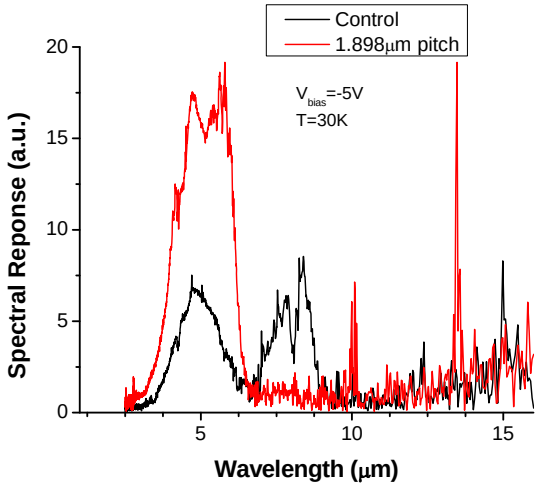

Fig 18: Spectral response from a sample with a patterned metal post structure with that of the control sample. A clear suppression of the LWIR peak is observed in this sample.

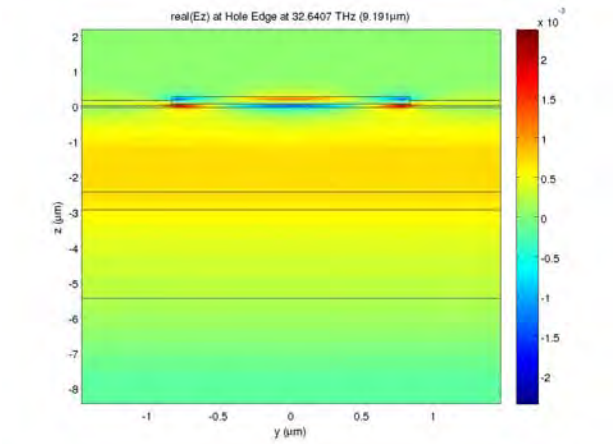

Fig 19: Y-Z mode profile of the fundamental mode of absorption in a metallic post pattern with Silver as the top metal. The mode is primarily concentrated away from the metal-semiconductor interface.

4. CONCLUSIONS:

During the last four years, there was a significant effort on developing quantum dot based focal plane arrays with plasmonic resonators. We have obtained very promising results on plasmonic enhancement in 320x256 focal plane arrays. The results from this work were submitted to Nature Communications. In addition, close collaboration was undertaken with Dr. John Hubbs and the RVSS group led by Allan Hahn. Vince Cowan (an AFRL employee), working on his doctoral dissertation with Prof. Krishna, successfully defended his PhD proposal.

Appendix: Related Publications

1. Shenoi R. V., Attaluri R. S., Siroya A., Shao J., Sharma Yagya D., Stintz A., Vandervelde T.E., and Krishna S. ,"Low-strain InAs/InGaAs/GaAs quantum dots-in-a-well infrared photodetector," J. Vac. Sci. Technol. B 26(3) May/Jun 2008 , PP-1136-1139
2. Plis Elena, Myers S., Kutty M.N., Mailfert J., Smith E., Johnson S., and Krishna S., "Lateral diffusion of minority carriers in InAsSb-based nBn detectors," APPLIED PHYSICS LETTERS 97, (2010) P-123503.
3. Khoshakhlagh A., Jaeckel F., Hains C. Rodriguez J.B., Dawson L.R., Malloy K., and Krishna S., "Background carrier concentration in midwave and longwave InAs/GaSb type II superlattices on GaAs substrate," APPLIED PHYSICS LETTERS **97**, 2010, P-051109.
4. Plis E., Rodriguez J.B., Balakrishnan G., Sharma Y.,Kim H.S., Rotter T. and Krishna S., "Mid-infrared InAs/GaSb strained layer superlattice detectors with nBn design grown on a GaAs substrate," Semicond. Sci. Technol. 25, 2010, P-085010.
5. Lee S.C., Krishna S., and Brueck S.R.J., "Quantum Dot Infrared Photodetector Enhanced by Surface Plasma Wave Excitation," Optics Express, 17, 2009, P-23161.
6. Myers S., Plis E., Khoshakhlagh A., Kim H.S., Sharma Yagya, Dawson R.,Krishna S., and Gin A., "The effect of absorber doping on electrical and optical properties of nBn based type-II InAs/GaSb strained layer superlattice infrared detectors," APPLIED PHYSICS LETTERS 95, 2009, P-121110.
7. Kim H.S.,Plis E., Gautam N.,Myers S., Sharma Y., Dawson L.R., and Krishna S., "Reduction of surface leakage current in InAs/GaSb strained layer long wavelength superlattice detectors using SU-8 passivation," APPLIED PHYSICS LETTERS 97, 2010, P-143512.
8. Barve A., Shao J., Sharma Yagya D., Vandervelde Thomas E., Sankalp Krit, Lee Sang Jun, Noh Sam Kyu, and Krishna Sanjay, "Resonant Tunneling Barriers in

uantum Dots-in-a-Well Infrared Photodetectors," IEEE JOURNAL OF QUANTUM ELECTRONICS, VOL. 46(7), JULY 2010, P-1105.

9. Sharma Yagya D., Kutty M.N., Shenoi R.V., Barve A.V., Myers S., Shao J., Plis E., Lee S.J., Noh S., and Krishna S., "Investigation of multistack InAs/InGaAs/GaAs self-assembled quantum dots-in-double-well structures for infrared detectors," J. Vac. Sci. Technol. B 28 (3) , May/Jun 2010.
10. Kim H.S., Plis E.,Khoshakhlagh A.,Myers S., Gautam N.,Sharma Y.D., Dawson L.R., Krishna S., Lee S.J., and Noh S.K., "Performance improvement of InAs/GaSb strained layer superlattice detectors by reducing surface leakage currents with SU-8 passivation," APPLIED PHYSICS LETTERS, 96, 2010, P-033502.
11. Kutty M.N.,Plis E., Khoshakhlagh A., Myers S., Gautam N., Smolev S., Sharma Y.D.,Dawson R.L., Krishna S., Lee S.J., and Noh S.K., "Study of Surface Treatments on InAs/GaSb Superlattice LWIR Detectors," Journal of ELECTRONIC MATERIALS DOI: 10.1007/s11664-010-1242(2010): AFRL FA9453-07- C-0171, AFOSR FA9550-09-1-0231, and KRISSGRL Program. Focused ion beam SEM system supported by NSF GrantCBET 0723224.
12. Barve A.V., Rotter T., Sharma Y.D., Lee S.J., Noh S.K., and Krishna S.' "Systematic study of different transitions in high operating temperature quantum dots in a well photodetectors," Appl. Phys. Lett. 97, 2010, P-061105
13. Plis E., Myers S., Khoshakhlagh A., Kim H.S., Sharma Y., Gautam N., Dawson R.L., Krishna S., "InAs/GaSb strained layer superlattice detectors with nBn design," Infrared Physics & Technology 52, 2009, PP-335–339.
14. Khoshakhlagh A., Plis E., Myers S., Sharma Y., Dawson L.R, and Krishna S., "Optimization of InAs/GaSb type-II superlattice interfaces for long-wave (~8 μm)infrared detection," Journal of Crystal Growth, 311, 2009, PP-1901–1904.
15. Rosenberg J., Shenoi R.V., Krishna S., and Painter O., "Design of plasmonic photonic crystal resonant cavities for polarization sensitive infrared photodetectors," Optics Express, Vol. 18, Issue 4, 2010, PP-3672-3686.
16. Shenoi R.V., Rosenberg J.,Vandervelde T.E., Painter S.J., and Krishna S., "Multispectral Quantum Dots-in-a-Well Infrared Detectors Using Plasmon

Assisted Cavities," IEEE JOURNAL OF QUANTUM ELECTRONICS, VOL. 46(7), JULY 2010, P-1051.

17. Rosenberg J.,Shenoi R.V., Vandervelde T.E., Krishna S., and Painter O., "A multispectral and polarization-selective surface-plasmon resonant midinfrared detector," APPLIED PHYSICS LETTERS 95, 2009, P-161101.
18. Ramirez David , Shao J., Hayat M. M., and Krishna S., "Midwave infrared quantum dot avalanche photodiode," APPLIED PHYSICS LETTERS 97, 2010, P-221106.
19. Barve A.V., Lee S.J., Noh S.K., and Krishna S., "Review of current progress in quantum dot infrared photodetectors," Laser & Photon. Rev., 2009, PP-1–13.
20. Krishna Sanjay, "The infrared retina," J. Phys. D: Appl. Phys. 42, 2009, P-234005.
21. Barve A. , Shah S., Shao J., Vandervelde T.,Shenoi R.V.,Jang W., and Krishna S. , "Reduction in dark current using resonant tunneling barriers in quantum dots-in-a-well long wavelength infrared photodetector," Applied Physics Letters 93, 2008, P-131115.
22. Andrews J.R., Restaino S.R. , Vandervelde T., Brown J.S., Sharma Y.D., Lee S.J., Teare S.W., Reisinger A., Sundaram M., and Krishna S., "Comparison of Long-Wave Infrared Quantum-Dots-in-a-Well and Quantum-Well Focal Plane Arrays," IEEE TRANSACTIONS ON ELECTRON DEVICES, VOL. 56, NO. 3, MARCH 2009, PP-512-516.
23. Jang W.Y. , Hayat M.M. , Tyo J.S., Attaluri R.S., Vandervelde T.E., , Sharma Yagya, Shenoi R.V., Stintz A., Cantwell E.R., Bender S.C., Lee Sang Jun , Noh S.K., and Krishna S., "Demonstration of Bias-Controlled Algorithmic Tuning of Quantum Dots in a Well (DWELL) MidIR Detectors," IEEE JOURNAL OF QUANTUM ELECTRONICS, VOL. 45, NO. 6, JUNE 2009, PP-674-683.
24. Plis E., Kim H.S., Bishop G., Krishna S., Banerjee K., and Ghosh S., "Lateral diffusion of minority carriers in nBn based type-II InAs/GaSb strained layer superlattice detectors," Appl. Phys. Lett. 93, 2008, P-123507.

25. IH.S., Plis E., Rodriguez J.B. , Bishop G., Sharma Y.D. and Krishna S., "N-type ohmic contact on type-II InAs/GaSb strained layer superlattices," ELECTRONICS LETTERS Vol. 44 No. 14 3rd July (2008) PP-881-882.

26. Martyniuk P., Krishna S., and Rogalski A., "Assessment of quantum dot infrared photodetectors for high temperature operation," JOURNAL OF APPLIED PHYSICS 104, 2008, P-034314.

27. Vandervelde T., Lenz M., Varley E., Barve A., Shao J., Shenoi R.V., Ramirez D., Jang W. , Sharma Y.D., and Krishna S., "Quantum Dots-in-a-Well Focal Plane Arrays," IEEE JOURNAL OF SELECTED TOPICS IN QUANTUM ELECTRONICS, VOL. 14, NO. 4, JULY/AUGUST 2008, PP-1150-1161.

28. Kim H.S., Plis E., Rodriguez J.B., Bishop G., Sharma Y.D., Dawson L.R., Krishna S., Bundas J., Cook S., Burrows D., Dennis R., Patnaude K., Reisinger A., and Sundaram M., "Mid-IR focal plane array based on type-II InAs/GaSb strain layer superlattice detector with nBn design," Appl. Phys. Lett. 92, 2008, P-183502.

29. Prasankumar R.P., Attaluri R.S., Averitt R.D., Urayama J., Weisse- Bernstein N., Rotella P., Stintz A., Krishna S., and Taylor A.J., "Ultrafast carrier dynamics in an InAs/InGaAs quantum dots-in-a-well heterostructure," OPTICS EXPRESS Vol. 16, No. 2, 2008, P-1165.

30. Rao T.V.C., Antoszewski J., Faraone L., Rodriguez J.B., Plis E., and Krishna S., "Characterization of carriers in GaSb/InAs superlattice grown on conductive GaSb substrate," APPLIED PHYSICS LETTERS 92, 2008, P-012121.

31. Varley E., Lenz M., Lee S.J., Brown J.S., Ramirez D.A., Stintz A., Krishna S., Reisinger A., and Sundaram M., "Single bump,two-color quantum dot camera", APPLIED PHYSICS LETTERS 91, 2007,P-081120.

DISTRIBUTION LIST

DTIC/OCP
8725 John J. Kingman Rd, Suite 0944
Ft Belvoir, VA 22060-6218 1 cy

AFRL/RVIL
Kirtland AFB, NM 87117-5776 2 cys

Official Record Copy
AFRL/RVSS/Leslie Vaughn 1 cy

(This page intentionally left blank)